OPTIMIZATION AND CONTROL OF PRESSURE SWING ADSORPTION SYSTEMS

Harish Khajuria, Efstratios N. Pistikopoulos*
Centre for Process System Engineering, Department of Chemical Engineering,
Imperial College, South Kensington Campus, London, SW7 2AZ, UK

Abstract

The real-time periodic performance of a pressure swing adsorption (PSA) system strongly depends upon the choice of key decision variables and operational considerations such as processing steps and column pressure temporal profiles, making its design and operation a challenging task. This work presents a detailed optimization based approach for simultaneously incorporating PSA design, operational and control aspects under the effect of time variant and invariant disturbances. For a two-bed, six-step PSA system represented by a rigorous mathematical model, the key optimization objective is to maximize the expected H_2 recovery while achieving a closed loop product H_2 purity of 99.99 %, for separating 70 % H_2, 30 % CH_4 feed. It is shown that incorporation of explicit/multi-parametric model predictive controllers improves the closed loop performance.

Keywords

Pressure swing adsorption, dynamic optimization, design under uncertainty, control, explicit MPC

Introduction

Pressure swing adsorption (PSA) is at the forefront of gas separation technology. In addition to handling multi-component separation and purification, PSA offers great flexibility at the operational stage, requiring careful selection of important decision variables. Further challenges are posed by the fact that the PSA operation is periodic in nature and never attains a true steady state.

The traditional approach for design of such process systems usually employs a two step sequential based method (first design, then control). In the last few decades, the importance of incorporating real-time operability aspects during the design stage itself has been greatly emphasized. Some of the early contributions in this field (Skogestad and Morari, 1987), albeit focusing on simplified linear systems provided various analytical tools towards integrated design and control formulations. A exhaustive survey of major contributions can be found in (Sakizlis et.al., 2004). An important trend which has emerged from the past studies is the wide acceptance of optimization based methods (Mohideen et.al., 1996; Bansal et.al., 2000; Moon et.al., 2011) and their applications to various systems such as distillation columns, CSTRs and systems represented by reduced models (Ricardez-Sandoval et.al., 2011). The application of optimization based approaches to inherently dynamic and highly nonlinear system like PSA still remains a challenging task. This is the main focus of this study, with particular interest in exploring the effects of PSA decision variables such as the duration of processing steps, on the operability of the system, and the appropriate design of its control system.

A key difficulty in the employment of optimization based approaches for PSA is to overcome the numerical computation and robustness issues encountered while

* To whom all correspondence should be addressed

employing a model which mimics the highly nonlinear and inherent dynamic nature of PSA operation. Most past studies have focused on the acceleration of cyclic steady state (CSS) to minimize the computational load related to the optimization procedures, including the complete discretization approach by Nilchan and Pantelides (1998), unibed approach (Kumar et.al., 1994; Nikolić et.al., 2009), and the direction determination approach by Jiang et.al. (2004). In this work, the traditional dynamic optimization approach was considered as more suitable for control studies and is employed, where the model is integrated in time towards a slow but true evolution to the CSS.

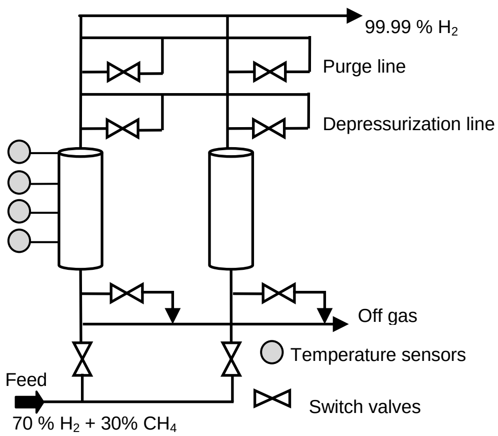

BED1	DEP	BLDN	PURGE	PE	REPRES	FEED
BED 2	PE	REPRES	FEED	DEP	BLDN	PURGE

Figure 1. Two bed, six step PSA system employed in this study.

Problem Description and Details

Figure 1 depicts a graphical overview of the two bed PSA system under consideration. Each bed is undergoing a cyclic operation comprising six processing steps and contains activated carbon as the adsorbent. Furthermore, it is also assumed that the structure of PSA cycle and sequence of processing steps remains fixed for the purpose of optimization studies. The detailed, first principle based dynamic model of PSA employed in this work is an extended version of previous work done by Khajuria and Pistikopoulos (2011). Its main features are showed in Table 1.

Objective Function

A popular objective function for PSA optimization seems to be product recovery due its direct relation to the plant operating cost. However, this is under the assumption that the PSA feed is already available at high pressure and does not require considerable compression work. In some cases, especially in air separation for O_2 and N_2 production, where the feed (air) is only available at atmospheric pressure, recovery alone is not a true indicator of PSA operating performance, and PSA overall compression work can also play a significant role. On the other hand, the key controller objective is to fast track the closed loop product purity to its desired set point in the event of process disturbances (Bitzer, 2002; Khajuria and Pistikopoulos, 2011). In a PSA operation, since recovery and purity vary in opposite direction (Khajuria and Pistikopoulos, 2011) with respect to important decision variables, a simultaneous optimization and control strategy appears to be an ideal platform to incorporate the impact of these two conflicting objectives on the real-time PSA performance. In this study, an optimal PSA operational policy and controller configuration is desired which provides the maximum value of closed loop hydrogen recovery while obeying all operational constraints, for the separation of 70 % H_2 and 30 % CH_4 feed mixture to a product stream of hydrogen purity greater than 99.99 %, in the presence of the following disturbances and uncertainty.

i. Feed temperature variations in a sinusoidal fashion with decaying amplitude
ii. Step increase in PSA feedrate by 0.35 Nm^3/hr
iii. Bounded uncertainty in the hydrogen feed composition, varying from 68 % to 73 %.

For providing the controller action, a SISO PI controller (Eq. (1)) is assumed, where purity is the control variable and feed step duration is considered as the manipulative variable (Khajuria and Pistikopoulos, 2011). Furthermore, integral square error (ISE) of purity, defined in Eq. (2), is treated as the controller performance indicator.

$$\begin{aligned} & t_{feed}(k) = t_{feed}(k-1) + K_c(1+\frac{T_s}{\tau_I})e(k) - K_c e(k-1) \\ & e(k) = 10^5(Purity(k) - 99.99) \\ & t_{feed}^{low} \le t_{feed}(k) \le t_{feed}^{up} \\ & \Delta t_{feed}^{low} \le \Delta t_{feed}(k) \le \Delta t_{feed}^{up} \end{aligned} \tag{1}$$

$$ISE = 10^5 \int_0^{t_f} (Purity(t) - 99.99)^2 dt \tag{2}$$

Here, t_{feed} is the time duration of the feed step in seconds, k is the sampling instant, T_s is the sampling interval which is assumed to be one PSA cycle, while Kc and τ_I are the proportional gain and integral time constant for the PI controller, respectively.

Decision Variables

A number of decision variables related to PSA process design, cycle scheduling and controller design should be selected carefully in order to obtain an optimal performance. The key process design variables considered are the column length, column diameter and valve CVs, while feed rate is included as an operational decision variable. The key PSA schedule variables considered are the time durations of the process steps of the underlying

PSA cycle, as they directly control the extent of related governing physical phenomena, determining the PSA key performance indicators such as recovery, purity and other operational constraints. Figure 1 shows that out of the time duration variables of the six processing steps, only three can be varied independently in order to maintain a synchronized PSA operational cycle. It is important to note that the optimal tuning of switch valves, by incorporating their CV as decision variable, is crucial to maintain suitable pressure-temporal profiles at the bed ends for varying bed dimensions and step durations. For the controller synthesis problem, manipulative variable bias value, controller gain and integral time are considered as decision variables.

Table 1. Key features of the PSA dynamic model

Individual component balance

$$(\varepsilon_b + (1-\varepsilon_b)\varepsilon_p)\frac{\partial C_i}{\partial t} + \frac{\partial UC_i}{\partial Z} + \rho_p(1-\varepsilon_b)\frac{\partial \bar{Q}_i}{\partial t} = \varepsilon_b D_Z \frac{\partial^2 C_i}{\partial Z^2}$$

Energy balance

$$\varepsilon_t \sum_{i=1}^{NCOMP} C_{v_i} C_i \frac{\partial T}{\partial t} + (1-\varepsilon_b)\rho_p \sum_{i=1}^{NCOMP} C_{v_i} \bar{Q}_i \frac{\partial T}{\partial t} + (1-\varepsilon_b) C_{p_s} \rho_p \frac{\partial T}{\partial t}$$
$$+ \left(\left(1+\frac{\Delta d_w}{D}\right)^2 - 1\right) C_{p_w} \rho_w \frac{\partial T}{\partial t} + U \sum_{i=1}^{NCOMP} C_{p_i} C_i \frac{\partial T}{\partial Z} - (\varepsilon_b + (1-\varepsilon_b)\varepsilon_p) RT \sum_{i=1}^{NCOMP} \frac{\partial C_i}{\partial t}$$
$$- (1-\varepsilon_b)\rho_p \sum_{i=1}^{NCOMP} \frac{\partial \bar{Q}_i}{\partial t}(-\Delta H_i) = \lambda \frac{\partial^2 T}{\partial Z^2}$$

Gas phase momentum balance

$$-\frac{\partial P}{\partial Z} = \frac{150\mu(1-\varepsilon)^2}{\varepsilon^3 d_p^2} U + \frac{1.75(1-\varepsilon)\sum_{i=1}^{NCOMP} C_i MW_i}{\varepsilon^3 d_p} |U| U$$

Multisite Langmuir Isotherm (Ribeiro, et al., 2008)

$$\frac{Q_i^*}{Q_i^{\max}} = a_i K_i C_i RT \left[1 - \sum_{i=1}^{NCOMP} \frac{Q_i^*}{Q_i^{\max}}\right]^{a_i}$$

$$K_i = K_{\infty_i} \exp\left(\frac{-\Delta H_i}{RT}\right)$$

LDF rate expression

$$\frac{\partial \bar{Q}_i}{\partial t} = K_{LDF_i}\left(Q_i^* - \bar{Q}_i\right)$$

Valve equation

$$U = \begin{cases} \phi C_V \sqrt{1-\left(\frac{P_{High}-P_{Low}}{P}\right)^2} & if\ \frac{P_{Low}}{P_{High}} < P_{critical} \\ C_V \frac{P_{High}}{P} & Otherwise \end{cases}$$

$$P_{critical} = \left(\frac{2}{1+\gamma}\right)^{\frac{\gamma}{1-\gamma}} \qquad \gamma = \frac{C_p}{C_v}$$

Operational Constraints

It should be noted that only providing purity violation information to the NLP solver can often lead to solutions where other important state variables may take values indicating unrealistic physical behavior during the time horizon of operation. One such consideration is the high values of fluid superficial velocity, especially during the flow reversal process steps including blowdown and repressurization with feed, which may result in fluidization of the bed. Another important consideration is the sharp rise of bed temperature during the first few PSA cycles in the adsorption stage. Bed temperatures beyond a certain limit, can be detrimental to the adsorbent activity and should be avoided. Consequently, such operational constraints are also incorporated in the overall optimization formulation. In this regard, to ensure that the hydrodynamic regime of the PSA is always under packed bed conditions, superficial fluid velocity at bed ends is constrained to be always less than the minimum fluidization velocity (Wen and Yu, 1966). Similarly, temperature at bed locations of Z/L = 0.25, 0.5, 0.75, 1 is constrained, as shown in Figure 1.

From real time control perspective, it is important to constraint both high and low values of adsorption time (Eq. (1)) to achieve a safe and economical operation. Very low values of feed step duration translates to shorter PSA cycles performing loading and unloading of the adsorbent with the impurities at a quicker rate, while significantly enhancing its degradation in the form of wear and tear. Furthermore, this also demands a faster ON and OFF operation of the switch valves, reducing their lifetime, which is directly related to number of switches per unit time. On other hand, long duration feed step can over saturate the bed, since the adsorbent has only a limited capacity for the impurities. In addition to this, large changes in the adsorption time (Δt_{feed}) should also be constrained to avoid over saturation (high Δt_{feed}) or avoid sudden surge of inflow (low Δt_{feed}). It is important to note that in general practice, the controller constraints mentioned in Eq. (1) can be treated as constraints in the original NLP problem itself. In this work, the explicit nature of the PI control law is exploited, and an IF-ELSE logic is built to incorporate these equations along with the general PDAE model of PSA. This approach enhances the convergence rates of the dynamic optimization problem without compromising its rigor.

A Framework for Simultaneous Design and Control Optimization of PSA Systems Under Uncertainty

In general, a system designed at the nominal conditions is liable to fail for small changes of uncertain conditions, in terms of constraint violations and performance degradation. To obtain an optimal PSA design which is operable under the full range of uncertain parameters, and known time varying disturbances, a rigorous and systematic approach (Mohideen et.al., 1996) is employed. The framework comprises the following three main steps.

Step 1 In this step, the uncertainty parameter, hydrogen feed composition, is discretized into a finite number of critical scenarios. Since its value can vary from 68 % to 73 %, three critical scenarios are chosen for discretization purposes. The first scenario corresponds to 73 % feed composition possibility with probability of 15

%, the second scenario correspond to hydrogen feed composition of 68 % with 15 % probability, while the third presents the nominal case of 70 % hydrogen composition with 70 % probability. The resulting simultaneous design and control optimization formulation is depicted in Eq. (3), where h_{d1} and h_{c1} are the equality constraints representing PSA model and controller description, respectively, while the decision variables are represented by d_P (process design), d_c (controller design), and v (operational), with θ being the parametric uncertainty.

$$\max_{d_P, d_c, v, t\in[0, t_f=50 cycles]} \sum_{m=1}^{3} w_{\theta_m} Rec_{H_2}(\theta_m)\Big|_{t_f}$$
$$s.t.$$
$$h_{d1}(\dot{xd}, xa, d_P, v, \theta_m, t)_m = 0 \quad m = 1,2,3$$
$$h_{c1}(\dot{xd}, xa, d_c, v, \theta_m, t)_m = 0 \quad m = 1,2,3$$
$$99.99 \le Pur_{H_2}(\theta_m, t_f)_m \le 100 \quad m = 1,2,3$$
$$0 \le ISE(\theta_m, t_f)_m \le \varepsilon_c \quad m = 1,2,3$$
$$0 \le U^i_{vio}(\theta_m, t_f)_m \le \varepsilon_c \quad i = 1,2 \quad m = 1,2,3$$
$$0 \le T^i_{vio}(\theta_m, t_f)_m \le \varepsilon_c \quad i = 1,2 \quad m = 1,2,3 \quad (3)$$

It should also be noted that ISE is treated as a constraint (Luyben and Floudas, 1994) (instead of being considered as a separate objective function), which makes ε_c a tuning parameter which can be changed to obtain a stable and fast controller response. Furthermore, the velocity and temperature violations, which usually act as path constraints are transformed to end point constraints via integrating their violation from their limiting values over time (Vassiliadis et. al., 1994). Here, the value of ε_c and ε_d are fixed at 2.2 and 10^{-5}, respectively.

Step 2 In this step, the multi-period dynamic optimization problem formulated in the last step is solved in gPROMS (PSE Ltd., 2010), with the modeling parameters listed in Appendix A. The resulting optimal decision variables and PSA performance indicators are shown in the Table 2, which shows that the maximum expected closed loop hydrogen recovery in this case comes out to be around 61 % for an expected value of ISE at 1.73.

Step 3 In this step, the dynamic feasibility test (Dimitriadis and Pistikopoulos, 1995) is performed to check whether the optimal design and control system obtained in the last step is feasible for the complete range of uncertain parameter. The dynamic feasibility test problem is formulated in the Eq. (4) below. Here, g_l represent the set of PSA inequality constraints, l is the constraint index, while Ncr is the total number of such constraints. If ψ is negative then the design is feasible for the operating range of uncertain parameter. If it is positive, then the design is infeasible and the critical scenario obtained from the complete solution of Eq. (4) is augmented with the list of critical scenarios described in ***Step 1***, and the whole procedure is repeated till feasibility is achieved.

$$\psi = \max_{l=1,..Ncr}\left[g_l(\theta^*) = \max_{\theta\in[68\%,73\%], t\in[0,t_f=50cycles]} g_l(\theta, t_f) \right] \qquad (4)$$

The value of ψ for the current design and control configuration comes out to be -0.6, with ISE as the limiting constraint. Since this is a negative value, the optimal PSA design obtained here is feasible and the algorithm terminates.

Table 2. Optimal decision variables, their upper and lower bounds and optimal performance variables for PSA optimization under uncertainty study

Decision variable	LB	UB	Value
Process design			
CV_{bldn}	0.065	1	0.0652
CV_{dep}	0.01	1	0.01025
CV_{repres}	0.06	1	0.06
CV_{purge}	7.7 X 10^{-5}	5 X 10^{-4}	5 X 10^{-4}
D(m)	0.05	0.5	0.1596
L/D	2	6	6
Operational			
Q^0_{feed} (Nm^3/hr)	0.5	1.7	1.699
t_{dep}(sec)	15	150	89.06
t_{repres} (sec)	30	150	34.512
Controller design			
$t_{feed}(t_0)$ (sec)	60	400	315.557
Kc	0.001	100	0.16334
τ_I	0.001	10^5	3.663
Performance variables for multi-period design (expected values)			
$E(Recovery_{H2})$	60.924 %	$E(Purity_{H2})$	99.99 %
$E(ISE)$	1.73		
Performance variables at y_{H2} = 70 %			
$Recovery_{H2}$	60.93 %	$Purity_{H2}$	99.99 %
ISE	1.688		

Remarks

From the results listed in Table 2, the following interesting observations can be drawn:

i. The duration of feed step is the largest as compared to other two steps. For the 2 bed, 6 step PSA cycle under consideration, where feed is provided in only one step (per bed) and then discontinued, this result seems quite logical, and can be attributed to the fact that it is during the feed step that actual recovery of product happens, which the optimizer attempts to maximize
ii. The system spends least amount of time in the pressurization/blowdown stage. This result appears to be in order with the fact that the system would like to quickly repressurize the column (from feed) in an attempt to minimize the impurity intake during this time, as well quickly depressurize (blowdown) the column to minimize the product losses through off gas.

Figure 2 depicts the complex interaction between the pressure swings, and the corresponding temperature swings for one complete PSA cycle, at CSS for the first bed. From this plot, it can been deduced that the temperature swing cycle is much slower to settle down as compared to pressure swing and also has an unfavorable effect on the PSA performance due to the temperature rise during the adsorption stages and drop during the desorption stages. Furthermore, it also shows that the repressurization at CSS is much faster than the blowdown, as the bed pressure at the end of blowdown stage has not reached the lowest pressure possible.

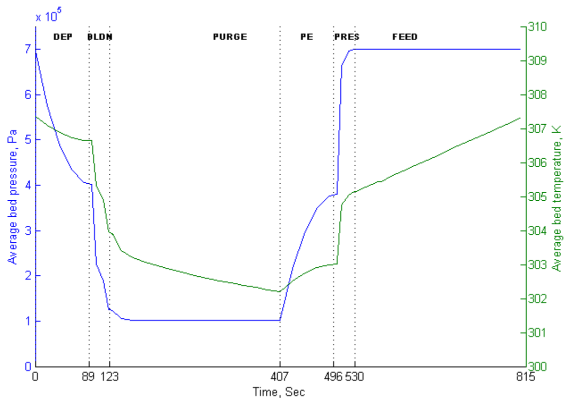

Figure 2. Time evolution of pressure swing and the associated temperature swing over a PSA cycle at the optimal conditions

Explicit/multi-parametric MPC for the nominal PSA design

At this point it appears worthwhile to investigate how a MPC controller would behave at the nominal conditions (Table 2).

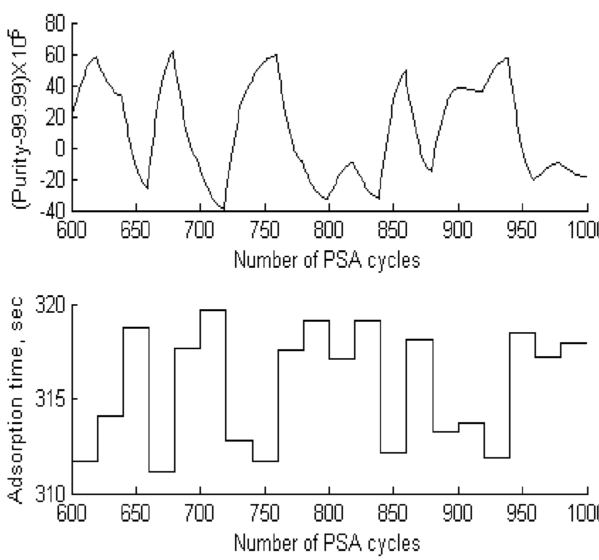

Figure 3. Purity response corresponding to the random variations in the manipulative variable

Recent advances made in the field of multi-parametric programming now makes it possible to obtain the governing MPC control law beforehand, or *offline* (Pistikopoulos et.al., 2000), leading to reduced online computations and other economic benefits (Pistikopoulos et.al., 2007; Pistikopoulos, 2009).

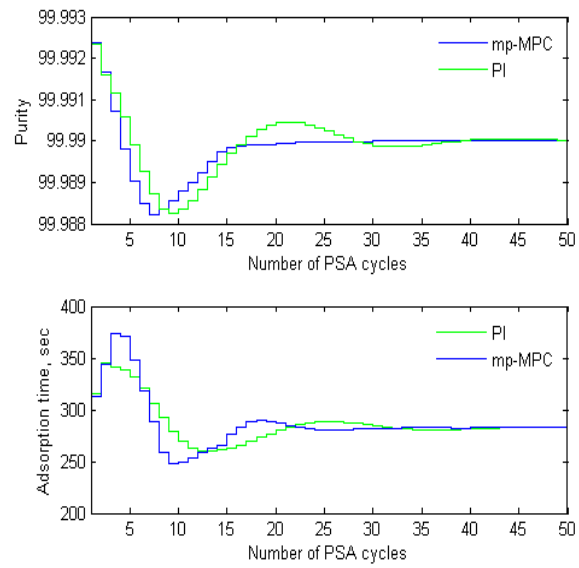

Figure 4. Comparison of closed loop performance for the PI and mp-MPC controller

Since, the large scale PSA model developed is not directly suitable for model based controller design; a system identification step (Ljung, 1987) is performed to identify a much simpler, preferably linear model relating the control variable, hydrogen purity with the manipulative variable, feed step duration to reasonable accuracy. The identification procedure followed in this study involves conducting dynamic simulations on the PDAE model, perturbed by a random pulse of input (feed step duration) disturbance in the open loop environment to ensure that the PSA system is excited *persistently* over a large frequency band (of interest). The resulting input-output response data (Figure 3) is used within the MATLAB system identification toolbox to identify the best fit linear parametric model, which is achieved for a 5^{th} order state space model with a mismatch of less than 5 % from the PDAE model response. A model based predictive controller (MPC), incorporating all controller constraints (Eq. (1)) in an optimization framework is formulated and the complete problem is solved through the POP toolbox in MATLAB, involving 8 parameters. The best value for tuning parameters is obtained by perturbing the original rigorous PSA model with time varying disturbances mentioned previously, and performing closed loop simulations. The resulting closed loop performance, for the best tuning parameters which also yields 101 critical regions, is shown in the Figure 4, along with the PI control performance. The comparison shows that the mp-MPC controller provides much more robust response in terms of less oscillatory behavior of the purity time trajectory. It is also important to note that the PI controller in this case is a special one as it considers all the system constraints, in a fashion similar to a mp-MPC controller. This appears to be main reason for the observation that the mp-MPC controller performance is not strikingly different from the PI case. The predictive power of the mp-MPC however, using the system dynamic model, seems to be the key feature for its slightly superior performance than the PI case.

Conclusions

This work presents a detailed study for the simultaneous design, operation and control of a PSA system following a rigorous and step by step built framework based optimization approach while utilizing a detailed mechanistic mathematical model. Important PSA operational challenges, constraints and objectives are discussed in detail and incorporated in the mathematical framework. The best closed loop recovery obtained for the PSA system under consideration is around 61 %, while handling multiple disturbance scenarios. Furthermore, a mp-MPC is also designed to observe any further benefits related to the model based controller. The results show improvement, albeit marginal, in the closed loop response with respect to the optimized PI controller considered in the study.

Appendix A. PSA simulation parameters

Product pressure	7 bars	Blowdown pressure	1 atm
Feed temperature	25^0 C	Particle diameter	3 mm
Bed porosity	0.4	Particle porosity	0.566

Acknowledgements

Financial support from the Royal Commission for the Exhibition of 1851, ParOS Ltd., EU project HY2SEPS (contract number: 019887), EPSRC (EP/G059071/1, EP/I014640/1), and KAUST is sincerely acknowledged.

References

Bansal, V.; Perkins, J.; Pistikopoulos, E.; Ross, R. & van Schijndel, J. (2000), 'Simultaneous design and control optimisation under uncertainty', Computers & Chemical Engineering 24(2-7), 261 - 266.

Bitzer, M. (2005), Model-based Nonlinear Tracking Control of Pressure Swing Adsorption Plants, in Thomas Meurer; Knut Graichen & Ernst-Dieter Gilles, ed., 'Control and Observer Design for Nonlinear Finite and Infinite Dimensional Systems', Springer Berlin / Heidelberg, , pp. 403-418.

Dimitriadis, V. D. & Pistikopoulos, E. N. (1995), 'Flexibility Analysis of Dynamic Systems', Industrial & Engineering Chemistry Research 34(12), 4451-4462.

Jiang, L.; Fox, V. G. & Biegler, L. T. (2004), 'Simulation and Optimal Design of Multiple-Bed Pressure Swing Adsorption Systems', AIChE Journal 50(11), 2904-2917.

Khajuria, H. & Pistikopoulos, E. N. (2011), 'Dynamic modeling and explicit/multi-parametric MPC control of pressure swing adsorption systems', Journal of Process Control 21(1), 151 - 163.

Kumar, R.; Fox, V. G.; Hartzog, D. G.; Larson, R. E.; Chen, Y. C.; Houghton, P. A. & Naheiri, T. (1994), 'A versatile process simulator for adsorptive separations', Chemical Engineering Science 49(18), 3115 - 3125.

Ljung, L. (1987), System Identification: Theory for the User, PTR Prentice Hall.

Luyben, M. & Floudas, C. (1994), 'Analyzing the interaction of design and control–1. A multiobjective framework and application to binary distillation synthesis', Computers & Chemical Engineering 18(10), 933 - 969.

Mohideen, M. J.; Perkins, J. D. & Pistikopoulos, E. N. (1996), 'Optimal Design of Dynamic Systems under Uncertainty', AlChE Journal 42(8), 2251-2272.

Moon, J.; Kim, S. & Linninger, A. A. (2011), 'Integrated design and control under uncertainty: Embedded control optimization for plantwide processes', Computers & Chemical Engineering 35(9), 1718 - 1724.

Nikolić, D.; Kikkinides, E. S. & Georgiadis, M. C. (2009), 'Optimization of Multibed Pressure Swing Adsorption Processes', Ind. Eng. Chem. Res. 48, 5388–5398.

Nilchan, S. & Pantelides, C. (1998), 'On the Optimisation of Periodic Adsorption Processes', Adsorption 4(2), 113-147.

Pistikopoulos, E. N. (2009), 'Perspectives in Multiparametric Programming and Explicit Model Predictive Control', AIChE Journal 55(8), 1918 - 1925.

Pistikopoulos, E. N.; Dua, V.; Bozinis, N. A.; Bemporad, A. & Morari, M. (2000), 'On-line optimization via off-line parametric optimization tools', Computers & Chemical Engineering 24(2-7), 188 - 188.

Pistikopoulos, E. N.; Georgiadis, M. C. & Dua, V. (2007), Multi-parametric Model-Based Control: Theory and Applications, Vol. 2, Wiley-VCH.

Rawlings, J. B. & Mayne, D. Q. (2009), Model Predictive Control: Theory and Design, Nob Hill Publishing.

Ricardez-Sandoval, L.; Douglas, P. & Budman, H. (2011), 'A methodology for the simultaneous design and control of large-scale systems under process parameter uncertainty', Computers & Chemical Engineering 35(2), 307 - 318.

Ruthven, D. M.; Farooq, S. & Knaebel, K. S. (1994), Pressure Swing Adsorption, Wiley-VCH.

Sakizlis, V.; Perkins, J. D. & Pistikopoulos, E. N. (2004), 'Recent advances in optimization-based simultaneous process and control design', Computers & Chemical Engineering 28(10), 2069 - 2086.

Skogestad, S. & Morari, M. (1987), 'Effect of disturbance directions on closed-loop performance', Industrial & Engineering Chemistry Research 26(10), 2029-2035.

Vassiliadis, V. S.; Sargent, R. W. H. & Pantelides, C. C. (1994), 'Solution of a Class of Multistage Dynamic Optimization Problems. 2. Problems with Path Constraints', Industrial & Engineering Chemistry Research 33(9), 2123-2133.

Wen, C. Y. & Yu, Y. H. (1966), 'A Generalized Method for Predicting the Minimum Fluidization Velocity', AIChE Journal 12(3), 610-612.

Process Systems Enterprise Ltd. (2010), gPROMS Model Developer Guide, ver. 3.3.1.